Chemical Science

ROYAL SOCIETY OF CHEMISTRY

EDGE ARTICLE

View Article Online
View Journal

Cite this: DOI: 10.1039/d6sc01541g

All publication charges for this article have been paid for by the Royal Society of Chemistry

Received 23rd February 2026
Accepted 20th May 2026

DOI: 10.1039/d6sc01541g

rsc.li/chemical-science

Pulsed electrolysis enables unexpected lactonization of bicyclobutane carboxylic acids

Anton S. Makarov, Liang Yi, Bholanath Maity, Luigi Cavallo * and Magnus Rueping *

Anodic oxidation of bicyclobutane carboxylic acids leads to unexpected lactonization and provides access to substituted benzene bioisosteres from highly strained precursors. High selectivity was achieved under pulsed electrolysis. Mechanistic experiments, supported by computational analysis, indicate that the transformation is initiated by single-electron oxidation of the substrate to form a bicyclobutyl radical cation, a key intermediate in redox-mediated transformations. These results demonstrate the utility of electrochemical methods for controlling the reactivity of bicyclobutane derivatives and provide a foundation for further development of sustainable oxidative transformations of strained molecules.

Introduction

Over the past decade, bicyclobutanes (BCB) have emerged as a versatile platform for targeting novel bicyclic scaffolds that expanded the chemical space for further exploratory research. Owing to a ring strain of 63.9 kcal mol^{-1},[1] BCBs readily undergo transformations ranging from cascade reactions triggered by electrophilic, nucleophilic, or radical addition to formal cycloadditions and spiroannulations delivering substantial increases in molecular complexity in a single operation.[2–5] Among the multitude of all-carbon- or heteroatom-containing bicyclic compounds that can be accessed from BCBs, decorated bicyclo[2.1.1]hexanes (BCHs) have been identified as valuable 3D surrogates for substituted benzenes, enabling bioisosteric replacement of aromatic rings that improve the pharmacokinetic profiles of respective small bioactive molecules (Fig. 1A).[6–8] As a consequence, efforts have been devoted to exploiting BCBs as precursors in synthetic routes not only to obtain functionalized BCHs but also to their heteroatom-containing counterparts with the goal of further tuning the physicochemical properties for downstream medicinal chemistry studies (Fig. 1B).[9–11]

Thermal formal [2σ + 2π]-cycloaddition had remained the primary method for converting BCBs to BCHs[12] until recently when the possibility to effectively promote the target reaction by Lewis acids with imines as 2π-components was reported.[13–15] The following years were marked by the development of conceptually new synthetic approaches to BCHs and their oxa- and aza-analogues. It has been demonstrated that BCBs, depending on the presence of certain functional groups, could be effectively transformed into (oxa/aza)-BCHs upon Brønsted-acid catalysis,[16,17] transition metal catalysis,[18,19] energy transfer catalysis,[20–23] or photoredox catalysis.[24–30]

In the past two years, BCB radical cations, resulting from the reductive quenching of an excited photocatalyst, have been proposed as important reactive intermediates in the construction of BCH derivatives (Fig. 1C).[24–27] Conceptually, electrochemical activation of BCBs offers a powerful and sustainable

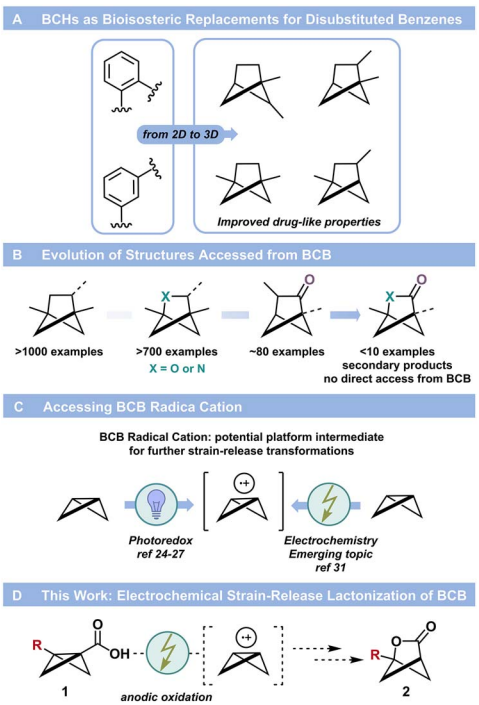

Fig. 1 Background and this work.

KAUST Catalysis Center (KCC), King Abdullah University of Science and Technology (KAUST), Thuwal 23955-6900, Saudi Arabia. E-mail: luigi.cavallo@kaust.edu.sa; magnus.rueping@kaust.edu.sa

route to these species. To date, however, only a single precedent has emerged: the work of Werz, who recently employed direct electrochemical formation of BCB radical cations in cycloaddition with aldehydes and arylation with arenes.[31,32]

As part of our ongoing interest in both electrochemical transformations[33–35] and the chemistry of strained compounds,[36,37] we aimed at studying the chemistry of BCBs under electrochemical conditions. Specifically, our objective was to examine radical intermediates formed through a decarboxylative approach. However, during our initial experiments, we accidently discovered that BCB acids **1** could be transformed into oxabicyclo[2.1.1]hexan-3-ones **2** upon electrolysis in an undivided cell (Fig. 1D). Considering that the observed process might represent another example of direct electrochemical activation of BCB *via* potential formation of its radical cations, which provides access to a novel class of oxa-BCHs,[38,39] we decided to investigate the reaction in greater detail.

Results and discussion

We commenced our studies by optimizing the electrolysis conditions for converting a model substrate **1a** into bicyclic lactone **2a** (Table 1). Following extensive experimentation, we established preliminary conditions using acetonitrile as the solvent, tetrabutylammonium bromide (TBAB) as the electrolyte, and a platinum anode. With either a platinum or stainless steel cathode, substrate **1a** was converted to product **2a** in 55% analytical yield accompanied by formation of bromolactone **3a** under electrolysis at 6 mA with a charge of 3 Faradays per mole. (Entries 1, 2). To our disappointment, these results showed limited reproducibility with respect to the formation of lactone **2a** as well as to **2a**/**3a** ratio.

Switching to a higher current density at the anode led to a notable increase in the yield of compound **2a**, although the issue of poor reproducibility persisted (Entries 3, 4). Higher current density, which typically leads to higher overpotential, may favor faster initial electron transfer to form the BCB radical cation, thereby improving the yield. However, under direct electrolysis conditions, this may lead to faster depletion of the substrate near the anode causing initial oxidation to become limited by mass transport. Poor mass transport, in turn, may cause overoxidation of the substrate. Combination of the aforementioned factors might be responsible for high discrepancy in the reaction performance. In the attempt to improve the reproducibility, we switched to a pulse technique as recently pulsed electrolysis had been shown to outperform direct

Table 1 Key optimization results[a]

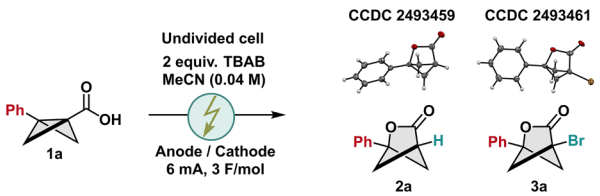

A Direct electrolysis, power supply[a]

Entry	Electrodes: anode/cathode	Yield of **2a**, %[b]	Yield of **3a**, %[b]
1	Pt plate (j = 3.0 mA cm^{-2})/SS[c] rod (j = 4.3 mA cm^{-2})	55[d]	15[d]
2	Pt plate (j = 3.0 mA cm^{-2})/Pt plate (j = 3.0 mA cm^{-2})	55[d]	15[d]
3	Pt wire (j = 31.6 mA cm^{-2})/SS rod (j = 4.3 mA cm^{-2})	75[d]	10[d]
4	Pt wire (j = 31.6 mA cm^{-2})/Pt plate (j = 3.0 mA cm^{-2})	75[d]	10[d]

B Pulsed electrolysis, potentiostat[a,e]

Entry	Program: pulse, s/resting period, s	Yield of **2a**, %[b]	Yield of **3a**, %[b]
5	10/10	70	5
6	10/20	65	5
7	10/30	65	5
8	20/0.5	35	15
9	20/20	65	5
10	20/30	80[f] (78)[g]	5
11	5/20	35	15
12	2/3	70	5

[a] Reaction scale – 0.1 mmol; cell dimensions, electrode geometry and other reaction parameters are described in the SI. [b] NMR yield, internal standard = CH_2Br_2. [c] SS stands for stainless steel. [d] Highest observed yields. [e] Pt wire (j = 31.6 mA cm^{-2}) served as working electrode (anode); Pt plate (j = 3.0 mA cm^{-2}) served as a counter electrode. [f] Reproduced five times in a raw, averaged analytical yield of **2a** was 80 ± 5%. [g] Isolated yield in parenthesis, 0.2 mmol scale, concentration – 0.08 M.

electrolysis in terms of selectivity and reproducibility in particular cases.[40,41] Indeed, pulsed electrolysis improved the reaction outcome: the sequence comprising a 10 s pulse followed by a 10 s resting period afforded lactone **2a** along with its brominated congener **3a** in 70% and 5% yields respectively in a consistent manner (Entry 5). By further varying the durations of the pulses and resting periods (Entries 6–9), we identified an optimal sequence that furnished high isolated yields of lactone **2a** with minimal formation of bromide **3a**, namely, a 20 s pulse followed by a 30 s resting period (Entry 10).

As a next step in our study, we examined the applicability of established reaction conditions to other substrates among the class of substituted BCB acids (Table 2). BCB acids bearing *para*-substituents on the aromatic ring were generally converted smoothly to the corresponding α-H-lactones **2b–g**. No pronounced dependence on electronic effects was observed, and substrates containing electron-withdrawing groups performed comparably to electron-neutral analogues.

For most of these reactions, the competing α-Br-lactones **3** were formed only in minor amounts (<10% analytical yield). A similar trend was found for *meta*-substituted derivatives. Most of these substrates afforded the desired lactones **2h–n** in good yields; the only exception was **2l**, which was obtained in 45% yield. The method also tolerated alkyl substitution at the bicyclic core, as demonstrated by the efficient formation of the homobenzyl-substituted lactone **2o** in good yield. Despite the preference for α-H-lactone formation, several substrates were transformed toward the α-Br lactones **3b–e.**

To gain a better understanding of the reaction, we performed a series of mechanistic experiments (Fig. 2). To assess the influence of potential local pH changes during electrolysis on the substrate,[42] we treated compound **1a** with either an acid or

Table 2 Scope of the reaction[a,b,c]

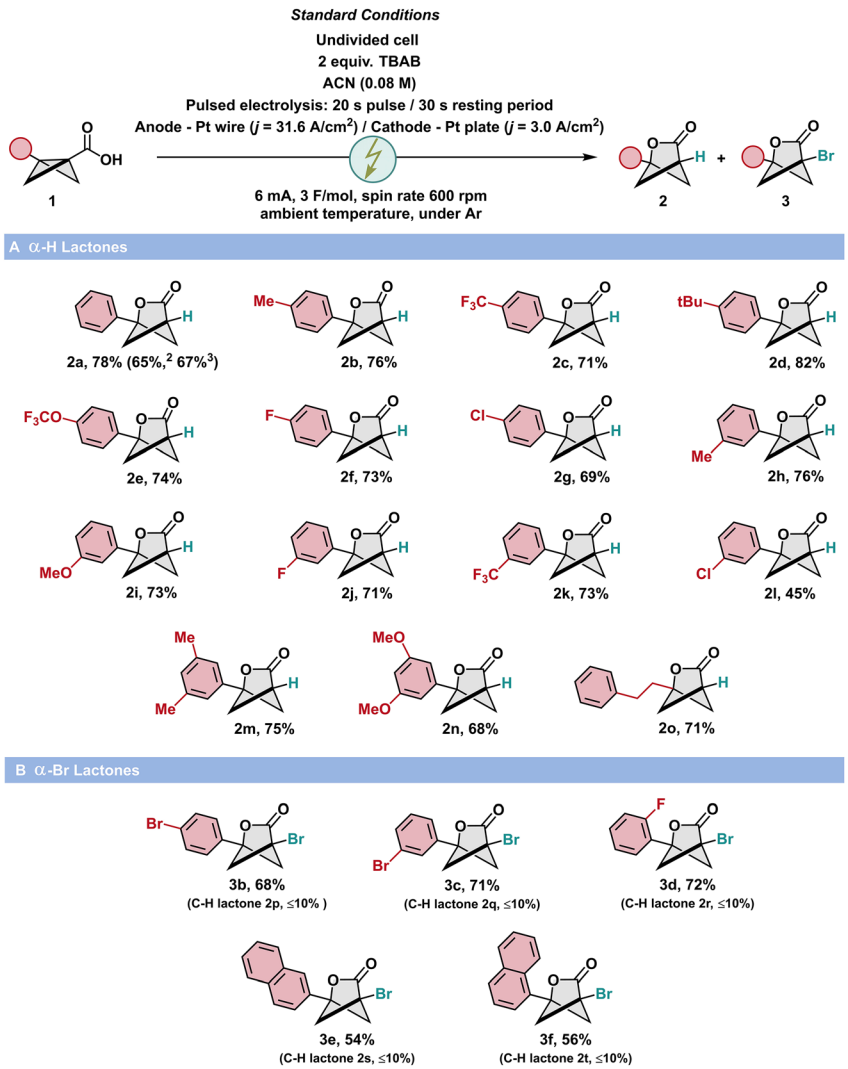

[a] Reaction scale – 0.2 mmol, yields refer to isolated yields after column chromatography. [b] Yield of **2a** at 0.5 mmol scale (concentration 0.13 M). [c] Yield of **2a** at 1.0 mmol scale (concentration 0.06 M).

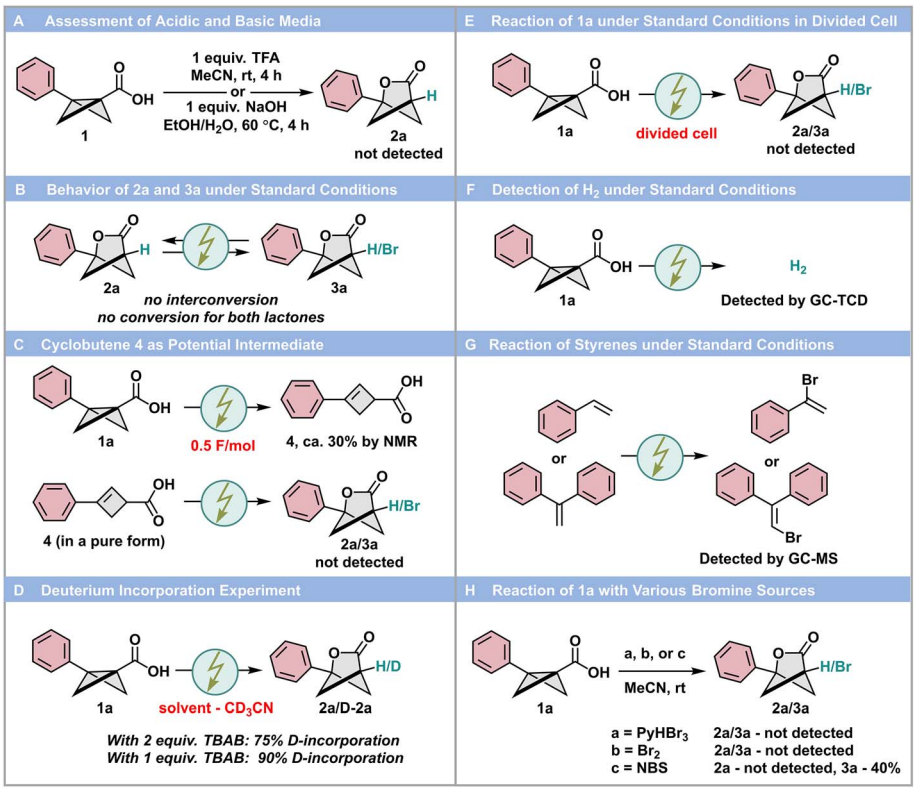

Fig. 2 Mechanistic studies of lactonization of bicyclobutane carboxylic acids.

a base (Fig. 2A). In both cases, lactone **2a** was not detected, which rules out the possibility that the key reaction is triggered by protonation or by reaction of the carboxylate anion. Lactone **2a** did not convert into bromolactone **3a** under the standard conditions, nor was bromolactone **3a** converted into lactone **2a**, indicating that the two compounds are not intermediates of one another (Fig. 2B). Moreover, both compounds exhibited considerable stability under the standard conditions, with little to no conversion observed for either. When the reaction of **1a** was stopped before one equivalent of electrons had passed, cyclobutene **4** was detected in approximately 30% analytical yield, with the conversion of substrate **1a** around 40% (Fig. 2C). We obtained compound **4** in a pure form and subjected it to standard conditions, which resulted in complete decomposition of the reaction mixture. Apparently, cyclobutene **4** is unlikely to be involved in the key transformation but rather arises as a side product from a potentially long-lived intermediate that collapses into compound **4** if the reaction is halted prematurely. To determine the source of the α-hydrogen, we performed electrolysis of **1a** in deuterated acetonitrile (Fig. 2D). Under standard conditions (2 equiv. TBAB), the degree of deuterium incorporation was 75%, whereas in the presence of 1 equiv. TBAB, 90% incorporation was observed. These results suggest that the solvent (acetonitrile) serves as the primary hydrogen-atom source, with TBAB possibly acting as an auxiliary source. Electrolysis of **1a** in a divided cell did not lead to the formation of **2a** and **3a**, suggesting that the reaction occurring at the counter electrode (cathode) is crucial for the formation of these products (Fig. 2E). One possible cathodic reaction of substrate **1a** is proton reduction. Indeed, hydrogen was detected in the gas phase above the reaction mixture by GC-TCD during electrolysis (Fig. 2F). Electrolysis of styrene and 1,1-diphenylethylene under standard conditions led to the formation of trace amounts of respective brominated products (Fig. 2G). Apparently, electrooxidation of bromide anion in TBAB provides some electrophilic bromine species that might interfere with the target reaction.[43]

Treatment of compound **1a** with pyridinium perbromide ($PyHBr_3$) and molecular bromine led to the decomposition of the reaction mixture, whereas the reaction of substrate **1a** with NBS furnished bromolactone **3a** in 40% analytical yield (Fig. 2H). Results of the last two sets of control experiments suggest that electrophilic bromine species other than molecular bromine can be responsible for the formation of products **3**. Although it is known that molecular bromine is formed upon electrolysis of bromide anion-containing solutions, under standard reaction conditions, its concentration is seemingly low.[44]

To further elucidate the reaction mechanism, additional electrochemical experiments were conducted. Irreversible oxidation of **1a** occurs at E_{pa} = +1.60 V *vs.* saturated calomel electrode (SCE) according to cyclic voltammetry (Fig. 3A). In the presence of TBAB, the anodic wave corresponding to the oxidation of **1a** is still observable, leading us to conclude that TBAB does not act as an effective electron mediator in the key transformation. Chronopotentiometric data obtained under the

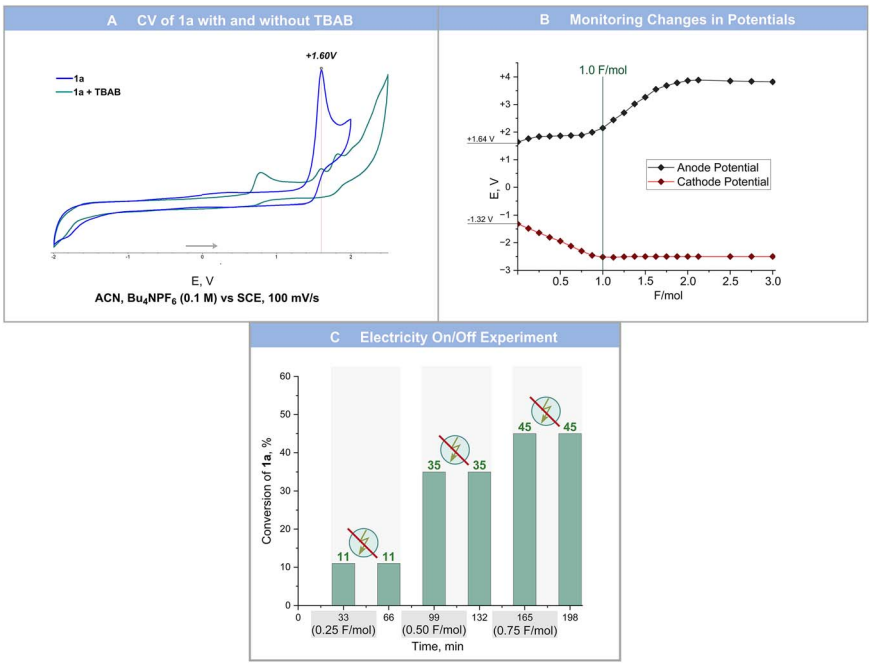

Fig. 3 Further mechanistic studies.

standard conditions showed that the process starts at an anodic potential of +1.64 V *vs.* SCE, nearly matching the oxidation peak potential of **1a** (Fig. 3B). The anodic potential increased only slightly until 1 F of charge had passed, after which it rose sharply to about +4.00 V *vs.* SCE, providing evidence for the initial oxidation of substrate **1a** during electrolysis. At the same time, the initial cathodic potential was measured at −1.32 V *vs.* SCE, decreasing to −2.50 V *vs.* SCE upon passage of 1 F of charge, where it remained until the end of the process, which might indicate there were a number of electrochemical reduction events involved at the beginning of the process. Results from the electricity on/off experiment indicate that substrate consumption is not driven by a chain process, as no change in conversion was observed during resting periods following each electrolytic step of 0.25 F mol^{-1} (Fig. 3C).

Supported by experimental observations, we performed density functional theory (DFT) calculations to establish a complete reaction mechanism. The calculated energetics along the proposed pathway are illustrated in Fig. 4. The reaction initiates with the single-electron oxidation of substrate **1a** at the anode, exhibiting a calculated redox potential of +0.22 V *vs.* Pt(111) electrode. This corresponds to +1.42 V *vs.* SCE, which aligns well with the experimental value (Fig. 3A). The generated radical cation **A** undergoes deprotonation at the cathode, releasing H_2 and forming intermediate **B** at −1.61 V *vs.* Pt(111). Natural population analysis indicates that the bridging bond in both **A** and **B** still exists, although it is weakened due to a one-electron interaction (Fig. S20 in SI). Subsequently, intermediate **B** undergoes cyclization to yield the α-radical lactone **C**, an endergonic process with an energy change of 3.7 kcal mol^{-1}. This step requires to overcome a free energy barrier of 20.8 kcal mol^{-1} *via* the transition state **B-TS**. A subsequent hydrogen atom transfer (HAT) from acetonitrile (solvent) to the radical carbon center of intermediate **C** produces the desired lactone product **2a**. This step is exergonic by 14.6 kcal mol^{-1}

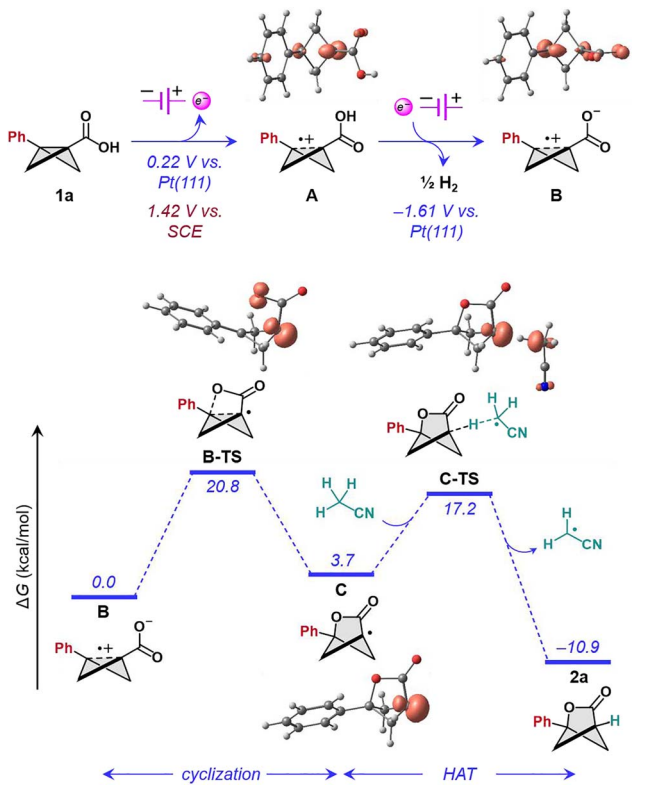

Fig. 4 DFT computed reaction mechanism. The reported energy values were calculated at ωB97xD(SMD, acetonitrile)/def2-TZVPP//ωB97xD(SMD, acetonitrile)/def2-SVP level of theory.

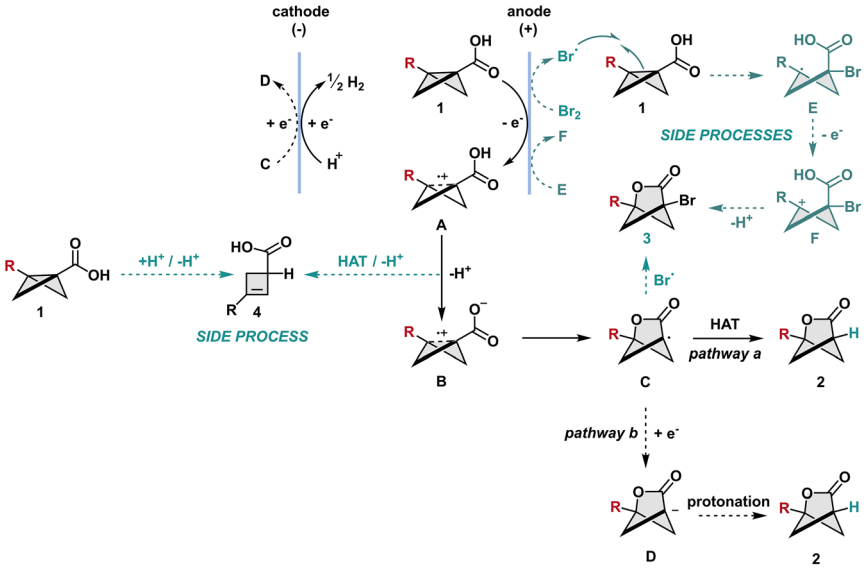

Fig. 5 Tentative mechanism.

and proceeds *via* transition state **C-TS** with a barrier of 13.5 kcal mol^{-1}. The calculations indicate that cyclization of **B** is the rate-determining step.

We also explored alternative reaction pathways with corresponding figures provided in the SI. One potential pathway considered the use of TBAB as the hydrogen atom donor for intermediate **C**: this route was determined to be kinetically less favourable by 1.1 kcal mol^{-1} compared to acetonitrile (Fig. S21 in the SI). These results suggest that TBAB can also function as an HAT agent. In another potential route, instead of undergoing HAT, intermediate **C** could undergo a single-electron reduction at the cathode with a calculated reduction potential of −1.99 V *vs.* Pt(111) (Fig. S22 in the SI), followed by a protonation by acetonitrile to yield the final product. Although this pathway offers no significant kinetic or thermodynamic benefit over the HAT process and involves a considerably lower reduction potential, provided the calculated potential at the cathode is reachable, this reduction pathway may become competitive with the HAT route. Nonetheless, the observation of bromolactones as byproducts provides indirect evidence supporting the HAT mechanism. The Br^- species undergoes single-electron oxidation at 0.23 V *vs.* Pt(111), forming an active $Br^{\bullet}$ radical, which subsequently couples with intermediate **C** to produce the bromolactone (Fig. S23 in the SI).

Based on experimental evidence and the results of computational studies, we propose the following mechanism for the devised transformation (Fig. 5). Anodic oxidation of acid **1** leads to a radical cation **A**, which, upon dissociation accompanied by a subsequent reduction of a proton, transforms into the respective carboxylate **B**. Intermediate **B** cyclizes into radical **C** followed by HAT from acetonitrile, and possibly from TBAB (pathway a) or undergoes electrochemical reduction with the formation of carbanion **D** that is protonated by the medium (pathway b). DFT calculations suggest that HAT pathway is more feasible. Cyclobutene **4**, in its turn, may arise either from deprotonation of intermediate **A** followed by HAT from acetonitrile/TBAB, or from proton-transfer-induced isomerization of substrate **1**. Bromolactones **3** could be formed upon direct attack of substrate **1** by electrochemically generated bromine radicals to form species **E** that undergo electrooxidation followed by cyclization. Alternatively, the formation of products **3** could result from recombination of bromine radicals with intermediate **C**.

Conclusion

In summary, we have shown that bicyclo[1.1.0]butane-1-carboxylic acids undergo electrochemically triggered lactonization to furnish 2-oxabicyclo[2.1.1]hexan-3-ones, representing a direct electrochemical activation of BCBs. The use of pulsed electrolysis provides an effective means to control chemoselectivity and to ensure reproducible outcomes. Mechanistic probes supported by computations indicate that the process starts with anodic oxidation leading to a bicyclobutyl radical cation susceptible to intramolecular carboxylate attack followed by hydrogen-atom abstraction or proton transfer from the medium. We anticipate that identified electrochemically enabled reactivity pattern will serve as a foundation for developing further sustainable electrosynthetic methodologies to convert BCBs into original architectures.

Author contributions

A. S. M. conceptualization, methodology, investigation, writing – original draft; L. Y. investigation; B. M. formal analysis, writing – original draft (computational part); L. C. supervision, writing – review and editing (computational part); M. R. conceptualization, project administration, supervision, writing – review & editing.

Conflicts of interest

There are no conflicts to declare.

Data availability

CCDC 2493459 (**2a**) and 2493461 (**3a**) contain the supplementary crystallographic data for this paper.[45a,b]

The data supporting this article have been included as part of the supplementary information (SI). Supplementary information is available. See DOI: https://doi.org/10.1039/d6sc01541g.

Acknowledgements

Financial support from King Abdullah University of Science and Technology (Awards No. ORFS-CRG12-2024-6438, REI/1/5246, URF/1/5063-01-01 and URF/1/6438) is gratefully acknowledged. We thank Dr. Jeremy Bau (KAUST) for consultations on the technical aspects of electrochemistry and Dr. Nursaya Zhumabay (KAUST) for assisting with hydrogen detection experiment.

Notes and references

1 K. B. Wiberg, *Angew. Chem., Int. Ed.*, 2003, **25**, 312.
2 Y. Koo, J. Jeong and S. Hong, *ACS Catal.*, 2025, **15**, 8078.
3 X. Liu, J. He, K. Lin, X. Wang and H. Cao, *Org. Chem. Front.*, 2024, **11**, 6942.
4 M. Golfmann and J. C. L. Walker, *Commun. Chem.*, 2023, **6**, 9.
5 C. B. Kelly, J. A. Milligan, L. J. Tilley and T. M. Sodano, *Chem. Sci.*, 2022, **13**, 11721.
6 J. Tsien, C. Hu, R. R. Merchant and T. Qin, *Nat. Rev. Chem*, 2024, **8**, 605.
7 A. Denisenko, P. Garbuz, S. V. Shishkina, N. M. Voloshchuk and P. K. Mykhailiuk, *Angew. Chem., Int. Ed.*, 2020, **59**, 20515.
8 F. Lovering, J. Bikker and C. Humblet, *J. Med. Chem.*, 2009, **52**, 6752.
9 V. V. Levterov, Y. Panasiuk, O. Shablykin, O. Stashkevych, K. Sahun, A. Rassokhin, I. Sadkova, D. Lesyk, A. Anisiforova, Y. Holota, P. Borysko, I. Bodenchuk, N. M. Voloshchuk and P. K. Mykhailiuk, *Angew. Chem., Int. Ed.*, 2024, **63**, e202319831.
10 A. Denisenko, P. Garbuz, N. M. Voloshchuk, Y. Holota, G. Al-Maali, P. Borysko and P. K. Mykhailiuk, *Nat. Chem.*, 2023, **15**, 1155.
11 V. V. Levterov, Y. Panasyuk, V. O. Pivnytska and P. K. Mykhailiuk, *Angew. Chem., Int. Ed.*, 2020, **59**, 7161.
12 P. Wipf and M. A. Walczak, *Angew. Chem., Int. Ed.*, 2006, **45**, 4172.
13 K. Dhake, K. J. Woelk, J. Becica, A. Un, S. E. Jenny and D. C. Leitch, *Angew. Chem., Int. Ed.*, 2022, **61**, e202204719.
14 L. Fan, P. Wang, C. He, X. Chen, L. Dai, D. Xiong and G. Zhong, *Chem. Sci.*, 2025, **16**, 18255.
15 R. S. Bitsch, E. Marcantonio, E. B. Obregon, I. R. Kocemba, J. Faghtmann and K. A. Jorgensen, *Chem. Sci.*, 2025, **16**, 16567.
16 J. T. Che, W. Y. Ding, H. B. Zhang, Y. B. Wang, S. H. Xiang and B. Tan, *Nat. Chem.*, 2025, **17**, 393.
17 L. Alama, N. Frank, L. Brucher, J. Nienhaus and B. List, *ACS Catal.*, 2025, **15**, 8297.
18 L. Zheng, Y. M. Yang, Z. P. Liu, W. Wang, W. J. Liang, H. L. Jiang, L. Yang, C. Lin, W. Su and J. A. Xiao, *Org. Lett.*, 2025, **27**, 229.
19 T. Li, Y. Wang, Y. Xu, H. Ren, Z. Lin, Z. Li and J. Zheng, *ACS Catal.*, 2024, **14**, 18799.
20 Y. C. Chang, M. Martin, K. Bortey, Q. Lefebvre, T. Fessard, C. Salome, R. J. Vazquez and M. K. Brown, *J. Am. Chem. Soc.*, 2025, **147**, 14936.
21 Y.-P. Cai, S.-R. Chen and Q.-H. Song, *Org. Chem. Front.*, 2025, **12**, 2676.
22 S. Dutta, Y. L. Lu, J. E. Erchinger, H. Shao, E. Studer, F. Schafer, H. Wang, D. Rana, C. G. Daniliuc, K. N. Houk and F. Glorius, *J. Am. Chem. Soc.*, 2024, **146**, 5232.
23 R. Guo, Y. C. Chang, L. Herter, C. Salome, S. E. Braley, T. C. Fessard and M. K. Brown, *J. Am. Chem. Soc.*, 2022, **144**, 7988.
24 S. Y. Tang, Z. J. Wang, J. J. Wu, Z. X. Xing, Z. Y. Du and H. M. Huang, *Chem. Sci.*, 2025, **16**, 11908.
25 J. L. Tyler, F. Schafer, H. Shao, C. Stein, A. Wong, C. G. Daniliuc, K. N. Houk and F. Glorius, *J. Am. Chem. Soc.*, 2024, **146**, 16237.
26 M. Golfmann, M. Reinhold, J. D. Steen, M. S. Deike, B. Rodemann, C. Golz, S. Crespi and J. C. L. Walker, *ACS Catal.*, 2024, **14**, 13987.
27 S. Dutta, D. Lee, K. Ozols, C. G. Daniliuc, R. Shintani and F. Glorius, *J. Am. Chem. Soc.*, 2024, **146**, 2789.
28 References 28-30 contain some selected non-classified contributions.A. Tena Meza, C. A. Rivera, H. Shao, A. V. Kelleghan, K. N. Houk and N. K. Garg, *Nature*, 2025, **640**, 683.
29 K. J. Woelk, K. Dhake, N. D. Schley and D. C. Leitch, *Chem. Commun.*, 2023, **59**, 13847.
30 S. Agasti, F. Beltran, E. Pye, N. Kaltsoyannis, G. E. M. Crisenza and D. J. Procter, *Nat. Chem.*, 2023, **15**, 535.
31 J. T. Maddigan-Wyatt, D. A. Knyazev and D. Werz, *Org. Lett.*, 2026, **28**, 2573.
32 For a recent example of an electrochemical transformation of BCB that does not involve the formation of BCB radical cation, see W.-Y. Zhang, X.-Y. Liu, Y. Li and J.-H. Li, *Green Chem.*, 2026, **28**, 2700.
33 H. Chen, C. Zhai, H. Zhang, C. Zhu and M. Rueping, *Nat. Commun.*, 2025, **16**, 7247.
34 C. Zhu, H. Chen, H. Yue and M. Rueping, *Nat. Synth.*, 2023, **2**, 1068.
35 H. Chen, C. Zhu, H. Yue and M. Rueping, *Angew. Chem., Int. Ed.*, 2023, **62**, e202306498.
36 L. Yi, D. Kong, A. P. Kale, R. Alshehri, H. Yue, A. Gizatullin, B. Maity, R. Kancherla, L. Cavallo and M. Rueping, *Angew. Chem., Int. Ed.*, 2024, **63**, e202411961.
37 L. Yi, A. S. Makarov, B. Maity, D. Kong, R. Alshehri, L. Cavallo, R. M. Koenigs and M. Rueping, *Angew. Chem., Int. Ed.*, 2026, **65**, e18508.

38 Such structures were generally accessed as products of postsynthetic transformations (references 36, 37) S. Tian, R. Liu, K. Zhang, Y. Xia, Y. Liu, P. Li, X. H. Duan and L. N. Guo, *Org. Lett.*, 2025, **27**, 3818.
39 C. C. Chintawar, R. Laskar, D. Rana, F. Schäfer, N. Van Wyngaerden, S. Dutta, C. G. Daniliuc and F. Glorius, *Nat. Catal.*, 2024, **7**, 1232.
40 F. De Bon, F. Lorandi, J. F. J. Coelho, A. C. Serra, K. Matyjaszewski and A. A. Isse, *Chem. Sci.*, 2022, **13**, 6008.
41 L. Zeng, J. Wang, D. Wang, H. Yi and A. Lei, *Angew. Chem., Int. Ed.*, 2023, **62**, e202309620.
42 M. C. O. Monteiro and M. T. M. Koper, *Curr. Opin. Electrochem.*, 2021, **25**, 100649.
43 P. P. Sen, V. J. Roy and S. R. Roy, *Green Chem.*, 2021, **23**, 5687.
44 L. G. Gombos and S. R. Waldvogel, *Sustainable Chem.*, 2022, **3**, 430.
45 (*a*) CCDC 2493459: Experimental Crystal Structure Determination, 2026, DOI: 10.5517/ccdc.csd.cc2ppn57; (*b*) CCDC 2493461: Experimental Crystal Structure Determination, 2026, DOI: 10.5517/ccdc.csd.cc2ppn79.